

BEP 8Z418

Coacervate-based protocells as a method for 14-3-3/tau stabilizer screening

Merel van den Bosch (1405152)

Many proteins do not function as a single molecular entity, but they will interact specifically with other proteins to form functional complexes. So called protein-protein interactions (PPIs) are essential for the functioning of the cell and therefore it is essential to study them. Stabilization of PPIs of 14-3-3 proteins has recently been under the attention of researchers as a drug target because of its many binding partners. However, these assays are usually performed in buffer solutions, which is not an accurate depiction of an *in vivo* scenario with the crowded cytosol of cells. In this work, amylose-based complex coacervates will be used to mimic the crowded environment of the cell's cytosol. It will be attempted to clear out the differences in PPIs of 14-3-3 and tau when a coacervate cell model is used compared to buffer solution and to investigate the possibility of using the model as a method for PPI stabilizer screening. Fluorescence polarization (FP) assays and confocal microscopy will be used for this. It is expected that the apparent K_D is lower in the protocell due higher local concentrations of the proteins and other molecules involved.

It has become clear that uptake of tau is influenced by the affinity of the 14-3-3 isoform used and that PPI in coacervates is stronger than in buffer solution. The K_D in the coacervate model was 100 fold lower than the K_D found in buffer solution. However, experiments showing any stabilization effect of deAcFC-A and aldehydes have not been successful yet.

Many proteins do not function as a single molecular entity, but they will interact specifically with other proteins to form functional complexes^[1]. So-called protein-protein interactions (PPIs) are essential for the functioning of the cell and therefore it is essential to study them. One example of PPIs in a pathophysiological context is the formation of neurofibrillary tangles (NFTs). Experiments focusing on PPIs are usually performed in buffer solutions, which is not an accurate depiction of an *in vivo* scenario with the crowded cytosol of cells.

Tau is a neural protein that carries out its function via the stabilization of microtubules. The protein contains 4 domains; an N-terminal projection, proline rich region, microtubule binding domain and a C-terminal region^[2]. The six tau isoforms differ from each other by the presence of either three or four repeat-regions in the C-terminal part of the molecule and the absence or presence of one or two inserts of 29 or 58 amino acids in the N-terminal part^[3]. Tau stabilizes microtubules under physiological conditions. However, under pathological conditions it forms into NFTs. The root cause of this is hyperphosphorylation of tau, since phosphorylation of tau enhances the formation of NFTs because tau's affinity for microtubules becomes lower when it is phosphorylated at multiple of 30 possible sites^{[3][4][5][6][7]}. Phosphorylation and expression of all isoforms of tau is increased under pathological conditions^[8] and this mainly happens at the proline rich region, but also at the N and C-terminal parts of the molecule. The NFTs form when tau aggregates into oligomers, these oligomers aggregate further into straight or paired helical filaments which will turn into NFTs. They are a primary biomarker for Alzheimer's disease (AD)^[9]. Phosphorylation might however not be the only mechanism behind their formation, since healthy fetal brain also contain phosphorylated tau proteins and non-phosphorylated tau proteins can also form filamentous structures under physiological conditions^[9]. Acetylation is suspected to influence NFT formation too^[10].

Tau interacts with 14-3-3 proteins, which are adapter proteins that have many binding partners and they are expressed in all eukaryotic cells^[4]. They regulate a multitude of signaling pathways including cell-cycle control, signal transduction, protein trafficking, and apoptosis through binding of kinases, proteases and transmembrane receptors^[11]. Their internal flexibility facilitates the recognition of many different proteins^[11]. They are especially abundant in the brain where they make up one percent of all soluble proteins. The 14-3-3 protein family consists of seven different isoforms (β , γ , ϵ , ζ , η , τ and σ) and they function as homodimers as well as heterodimers, except 14-3-3 σ , which preferentially forms homodimers^[12]. 14-3-3 can directly change the activity of proteins by changing their conformation or half-life, it can also serve as a platform to bring other proteins together to facilitate their interaction. Lastly, 14-3-3 can control protein trafficking by targeting specific amino acid sequences of target proteins. Five isoforms are present in the cytosol (β , ϵ , ζ , σ , and τ), 14-3-3 γ is predominantly found in the nucleus and 14-3-3 η can be found in mitochondria^[13]. The overall structure of 14-3-3 proteins is very well preserved throughout species, the differences in isoforms can mainly be found two flexible loops^[11]. At a molecular level, PPIs with the amphipathic groove of 14-3-3 are strongest when the peptide sequence RXXpZXP (X = any residue, pZ = phosphorylated S or T), is met^{[13][14][15]}. This motif is also present in the tau peptide. 14-3-3 ζ is abundantly present in the brain has been found to be present in NFTs. Furthermore, it is implicated in several neurological disorders, including schizophrenia, Alzheimer's disease and Parkinson's disease, which makes it a clinically

relevant protein to examine. It is suspected to be an effector for tau phosphorylation^[5]. Furthermore 14-3-3 γ levels are elevated in Alzheimer's disease^[12].

Phosphorylated tau at Ser 214 and 324 (ptau) interacts 10 folds stronger compared to non-phosphorylated tau^[16]. Non-phosphorylated tau does not form a stable complex with 14-3-3 while phosphorylated tau does and has a K_D in the low micromolar range^[4]. Each monomer of the 14-3-3 dimer can bind one of these two phosphorylated sites of tau (figure 1, right) which is essential for forming an aggregation resistant complex^[4]. Amino acids in 14-3-3 that are responsible for binding tau include Lys-49, Arg-56, and Arg-60 Val-176 and Leu at positions 216, 220, and 227. Furthermore, co-crystal structures of 14-3-3 with phosphopeptides suggest a role of Leu-120, Arg-127, Leu-172, Asn-173, Glu-180, Asn-224, and Trp-228^[17]. The mode of binding influences whether tau becomes more aggregation prone or aggregation resistant. The binding of non-phosphorylated tau to 14-3-3 was found to stimulate its aggregation in NFTs, this can be seen in figure 1 on the left^[18]. On the other hand, phosphorylated tau comes into an aggregation resistant state when bound to 14-3-3. Furthermore, 14-3-3 can compete with microtubules for tau binding due to its high concentration in the brain. Figure 1 demonstrates that the PPI of 14-3-3/ptau makes the protein aggregation resistant which could prevent the formation of NFT. This is why the stabilization of the ptau/14-3-3 PPI could be a potential therapeutic target in treating AD^[19].

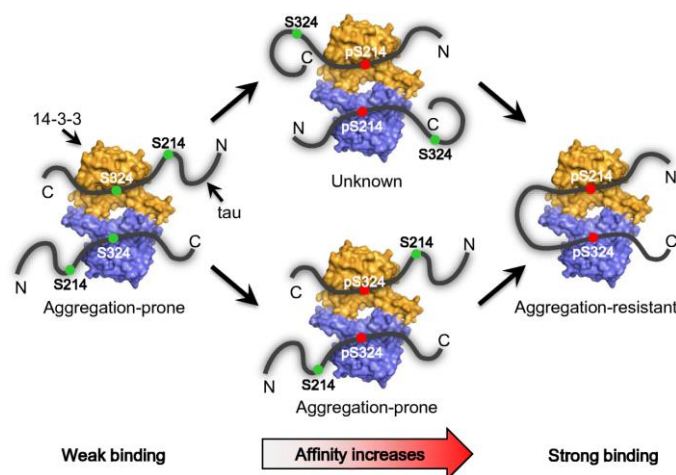


Figure 1 Schematic illustration of tau/14-3-3 interaction and propensity of aggregation. Specific interactions of tau and 14-3-3 are mediated by Ser214 (in the proline rich region) and Ser324 (in the microtubule binding domain) motifs on tau and the peptide binding grooves of 14-3-3. Phosphorylation of tau at these serines increases its binding affinity to 14-3-3 and changes the stoichiometry from 2:2 to 1:2 (tau:14-3-3 monomer) on the right. This shift in stoichiometry also switches the interaction with tau from aggregation prone to aggregation resistant^[20].

Previous research on this specific PPI has been performed in buffer solution but not yet in a more realistic cell model^{[13][20][4]}. Artificial cells are simplified models that resemble cells, they are composed from the bottom-up by non-living materials and allow specific facets of cell biology to be studied in a simplified environment where variables can be controlled^[21]. Apart from a bottom-up approach, artificial cells can be made by a top-down approach too. In this approach, non-essential genes are knocked out or replaced by synthetic genes to produce the artificial cell. There are also non-typical artificial cells, which mimic specific properties of biological cells such as shapes, morphology, or some functionalities^[22]. Artificial cells can be generated using multiple approaches, including bulk self-assembly and methods

using lipid vesicles^[23,24]. There has also been an increasing interest in the use of microfluidics to create them^[21]. Coacervate models are interesting to use because a cellular aspect that influences protein folding, function, stability and enzymatic reaction kinetics is molecular crowding. Up to 40% of the cellular environment is occupied by macromolecules^[25]. The molecular crowding of coacervate cell models allow the effects of this to be studied in controlled conditions.

An artificial cell method had been proposed by Altenburg et al. that uses biopolymer coacervate microdroplets. The cell-sized microdroplets arise through spontaneous self-assembly^[26] and form coacervates which are polymer-rich, cell-sized, crowded droplets, that show strong incorporation of cargo inside their core due to charge complementarity and/or hydrophobicity. This model stimulates the cell's cytosol and membrane. They were created via the method of Altenburg et al. via the coalescence of positively charged quaternized amylose (Q-Am) and negatively charged carboxymethylated amylose (Cm-Am). To stabilize the coacervate that is formed, a terpolymer is added. Uptake of macromolecules into the artificial cell required a negative charge. To overcome this limitation, amylose was functionalized with a Nitrilotriacetic acid (NTA) group, which coordinates Ni²⁺ and binds His-tagged proteins. A schematic overview of the production of these artificial cells can be seen in figure 2. A bulk concentration of a His-tagged protein of 250 nM was increased to 40 μ M in the coacervates^[27]. This higher local concentration can be compared to the localization of co-dependent molecules in cells to increase enzymatic activity. A higher enzymatic activity was also observed in the coacervates.

Different effects could change the PPI stabilization effect in coacervates. Previous research has shown that the relative association constants linearly change with the viscosity of the fluid. The slope should be 1 or less for a (partially) diffusion controlled interaction^[28]. Since the viscosity in the coacervates is higher, this could have a negative effect on the interaction and stabilization of the proteins. Furthermore, it has been shown that diffusivity of bio-macromolecules is decreased in the artificial cell model^[29]. Recent studies also suggest that soft interactions between proteins and crowders can destabilize PPI formation, opposing the normally assumed stabilizing effect of the crowded environment because of entropic-excluded volume effects^{[30][31]}

This study aims to investigate the difference in tau/14-3-3 stabilizer kinetics in the artificial cell model proposed by Altenburg et al. compared to buffer solution and find out whether this is a good platform for PPI stabilizer screening. Ultimately there will be a better insight into stabilizer kinetics in a cell-like environment. This goal will be achieved by performing fluorescence polarization (FP) assays and confocal microscopy.

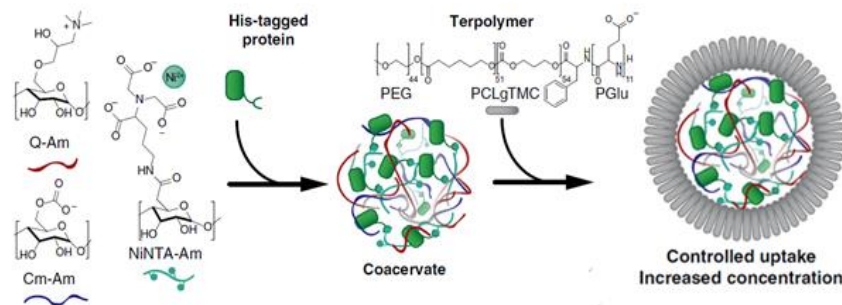


Figure 2 Coacervates are formed by the coalescence of positively charged Q-Am and negatively charged Cm-Am. Terpolymer is added to stabilize the coacervate and uptake of proteins is performed via amylose with an NTA group that coordinated Ni²⁺ and binds His-tagged proteins. Adapted from Altenburg et al.^[27]

¹ Laboratory of Chemical Biology, Department of Biomedical Engineering and Institute for Complex Molecular Systems, Eindhoven University of Technology, PO Box 513, Eindhoven 5600MB, The Netherlands. Correspondence and requests for materials should be addressed to M.v.d.B. (email: m.v.d.bosch@student.tue.nl or L.B. (email: l.brunsveld@tue.nl).

The 14-3-3 isoforms that will be used in this study are γ , ζ and σ because the γ isoform has the highest affinity for tau while σ has the lowest, so a clear image can be formed about the range of activity. 14-3-3 ζ is the most abundant in the brain and therefore clinically relevant. Surface plasmon resonance experiments have shown that the binding affinity of phosphorylated tau and 14-3-3 ζ is 22 nM^[32]. The interaction between phosphorylated 4R-tau and 14-3-3 σ is much weaker, it has been studied by NMR and a K_D of 6.5 μ M was found^[6]. The molecules that will be used for this are known stabilizers 3'-deacetyl fusicoccin-A (deAcFC-A) and aldehydes. FC-A is a diterpene that has been proven as a 14-3-3 stabilizer with phosphorylated proteins. FC-A enhances contacts between 14-3-3 proteins and their binding partner. FC-A binds to the hydrophobic cavity of 14-3-3 and it simultaneously interacts with the binding peptide^[33]. Previous research has shown that FC-A activity differs slightly between isoforms, the biggest difference was observed for 14-3-3 σ ^[13]. Aldehydes bind covalently to 14-3-3 via the formation of an imine bond with Lys122. This amino acid lies at the interface of the binding pocket formed by the protein complex, which lies adjacent to the phospho-accepting binding pocket where tau binds^[34]. A bivalent tau peptide will be used where the sequence RXXpZXP explained above is met.

Different effects might cause the stabilization effect to change between the tested conditions. It has already been shown that phosphorylated tau has a much higher affinity for 14-3-3 compared to non-phosphorylated^[4]. Keeping this in mind, the focus will be on phosphorylated tau first since this seems to have the most relevance and non-phosphorylated tau can be considered in later research. Furthermore, different 14-3-3 isoforms are tested and it is expected that the K_D of the γ isoform will be the lowest and that σ will have the highest with a K_D between 5 and 10 μ M^[6]. A distinction can also be made between monovalent and bivalent tau proteins where the difference between them can be assigned to a tethering effect. It is expected that bivalent peptides will interact stronger compared to monovalent peptides^[35].

The local concentration of proteins in the coacervate model is much higher than in buffer solution, this is expected to cause the stabilization effect to be stronger in the artificial cell model^[27]. Lastly, it is expected that the stabilization effect of aldehydes will happen over time since the covalent bond is not formed instantly and is kinetically controlled^[36]. This effect is expected in coacervates and in buffer solution, however the uptake of stabilizer into the coacervate is expected to slow down the effect compared to in buffer. All these effects might influence PPIs in coacervates, and this work sets out to find out how these effects interplay and contribute to PPIs in coacervates.

Results & discussion

The sequences of tau peptides and structures of compounds used apart from the 14-3-3 isoforms are shown in table 1. These two different tau peptides both have a different affinity for 14-3-3, tau peptide 2 binds much stronger than bivalent tau peptide 1. Both were used for some assays. Protein expression and purification was performed to produce the required 14-3-3 σ and 14-3-3 γ isoforms. Q-TOF and SDS-page analysis was performed on the expressed proteins. These results can be found in figure S 2, S3 and S4. An FP assay with bivalent tau peptide and 14-3-3 isoforms was carried out to determine their dissociation constants. The K_D of bivalent tau peptide 2 to 14-3-3 σ and 14-3-3 γ were determined to be $2.7 \pm 0.281 \mu\text{M}$ and $42 \pm 2.96 \text{ nM}$ respectively the assay results can be seen in figure S 1. The EC_{20} was set at 5 nM for 14-3-3 γ and 200 nM for 14-3-3 σ , compound titrations were performed at this 14-3-3 concentration.

Initial experiments were performed with the stronger binding bivalent tau peptide 2. Compound titrations were carried out to determine the apparent K_D 's of all compounds to the 14-3-3 isoforms, the results can be seen in figure S 5- S14. The K_D 's could not be determined since no S-curves were obtained. However, the anisotropy for the groups with compounds was higher than the control group, so it can still be concluded that there is a stabilization effect from these compounds. The assay should be optimized by using for example a weaker binding tau peptide. The increase in anisotropy for the group with 183 overtime indicates that it takes time for the imine bond to form between 14-3-3 and the aldehyde, this effect can however only be seen in the case of 14-3-3 σ and was not observed for 14-3-3 γ . This indicates that the kinetics of the reaction with the γ isoform are much quicker than for σ . The 188 group with only peptide and compound anisotropy increases at higher concentration, this indicates that the compound also interacts with the tau peptide, which is possible because an imine bond can be formed with the two lysines in the peptide. The high anisotropy increase gives the indication that the peptide aggregated due to this interaction. The increase in anisotropy for this group is also similar compared to the groups with 14-3-3. This result implies that the data from the interaction with 14-3-3 are not reliable, since the compound and peptide might cause the increase in anisotropy, and not just the binding of tau to 14-3-3. The affinity of deAcFC-A to 14-3-3 isoforms decreased overtime, which was not expected since the interaction between the molecules relies mostly on hydrophobic interactions which are not time dependent. An explanation for this could be degradation of deAcFC-A in the buffer, it should be

checked whether this is the case. These ambiguous data suggest that the experiments were not successful and that these assays should be optimized to obtain proper S-curves. This optimization could include using a different range of compound concentrations. Another remarkable result is that the 14-3-3 σ control group anisotropy increases overtime, which indicates that DMSO causes something in 14-3-3 σ in a way that it does not with 14-3-3 γ . DMSO at high concentrations can cause peptide and protein unfolding and thereby aggregation and this could explain the unexpected results^[37]. However, the result is inconsistent with previous research where concentrations DMSO up to ten percent were tolerated^[38]. Both 14-3-3 isoforms were titrated with a constant compound concentration, the results of the first assay using 183 can be found in figure 3. The groups with compound present had a lower apparent K_D than the intrinsic K_D of control groups, which confirms that 183 stabilizes the PPI, although this effect for 14-3-3 γ seems to be very small at $t=0$ and the effect observed for 14-3-3 σ is bigger, which is consistent with literature where the 14-3-3 σ form also had a larger stabilizing effect^[13]. It can be seen that the stabilization effect over time increases, since the difference in the K_D of groups with and without 183 becomes bigger, this was expected, it takes time for the equilibrium of this imine bond formation to be reached. Again, a side reaction seems to occur with 14-3-3 σ overtime, it is possible that the stabilizer reacts with other lysines in the protein or peptide that causes it to aggregate.

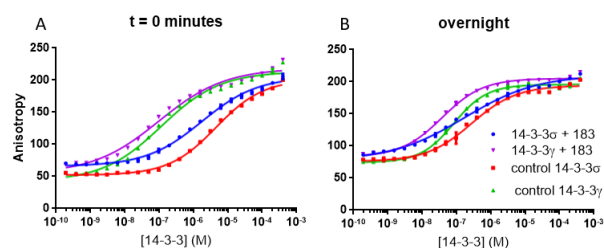


Figure 3 FP assay of a 14-3-3 σ and 14-3-3 γ titration measured at $t=0$ minutes (A) and overnight (B) with constant bivalent tau peptide 2 concentration (10nM) and constant 183 concentration (250 μM). Measured apparent K_D values at $t=0$ were for 14-3-3 σ 1.7 μM and 4.6 μM for the group with compound and DMSO control respectively. The values for 14-3-3 γ were 99 nM and 114 nM. The values measured overnight were for 14-3-3 σ were 168 \pm 17.3 nM and 273 \pm 21.1 nM for the group with compound and DMSO control respectively. The values for 14-3-3 γ were 37 \pm 2.34 nM and 82 \pm 3.59 nM.

This experiment was repeated for 14-3-3 γ with deAC-FC-A, 188 and 183, but this time the weaker binding tau peptide 1 was used. The results can be found in figure 4 and additional measurements can be seen in figures S 15-17. The stabilization effect of de-AC-FC-A can be seen right away. The aldehydes do not seem to have any effect at $t=0$ minutes yet, but their effect can clearly be seen overnight, which confirms that the covalent imine bond needs time to form. The effect of deAc-FC-A however, decreases slightly overtime. It should be tested whether the compound degraded in the buffer, this could explain these unexpected results.

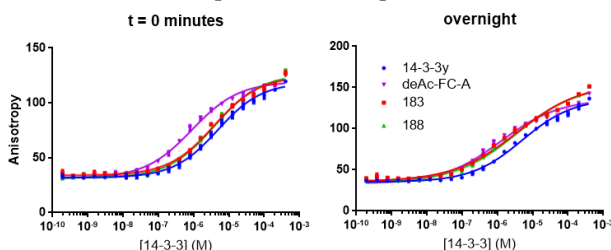
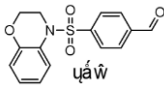
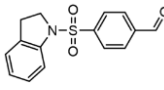
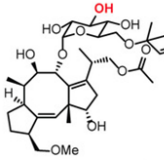


Figure 4 14-3-3 titration with 250 μM stabilizer concentration and one percent DMSO measured at $t=0$. The bivalent tau peptide 1 concentration was 100 nM. The apparent K_D 's were 4.7 \pm 0.369 μM , 3.8 \pm 0.299 μM , 3.8 \pm 0.314 μM and 0.88 \pm 0.065 μM for the groups without stabilizer, with 183, 188 and deAc-FC-A respectively. The values measured overnight were 4.9 \pm 0.584 μM , 3.6 \pm 0.632 μM , 3.5 \pm 0.496 μM and 1.2 \pm 0.176 μM for the groups without stabilizer, with 183, 188 and deAc-FC-A respectively.

Table 1 Peptide sequences and chemical structures of the compounds used

Name	Structure/peptide sequence
Bivalent tau peptide 1	RTP{pSER}LPTGGG SGGSGGGGSKCG{pSER}LGNIHHK
Bivalent tau peptide 2	SRTP{pSER}LPTPPTREGGGSGGGSGGGV TSKCG{pSER}LGNIHHK
183	
188	
3'deacetyl fusicoccin-A	

Next, the proteins were loaded in coacervates and investigated by confocal microscopy to assess protein uptake and localization in the coacervates. The confocal microscopy images in figure 5 showed that the method of producing the terpolymer stabilized coacervates was successful and the His-tagged 14-3-3 isoforms were both taken up into the coacervate. It was found that the driving force of the tau peptide entering the coacervate was its affinity with the 14-3-3 isoform. This can be concluded because only minimum uptake was observed when 14-3-3 σ was used in the coacervate and much more uptake of tau peptide was observed for 14-3-3 γ . This is why further coacervate experiments were performed with 14-3-3 γ , even though the stabilization effect of this isoform is the least according to literature^[13]. Full-length tau (GFP-tau) was also loaded in the coacervates since this could be an interesting point of future research. A remarkable finding was that tau-GFP without the presence of 14-3-3 localized at the membrane of the coacervate and that this did not happen when 14-3-3 was added. Tau has a relatively large amount of hydrophobic amino acids which might have interacted with the hydrophobic part of the terpolymer and therefore it did not diffuse further into the coacervates but localized at the membrane.

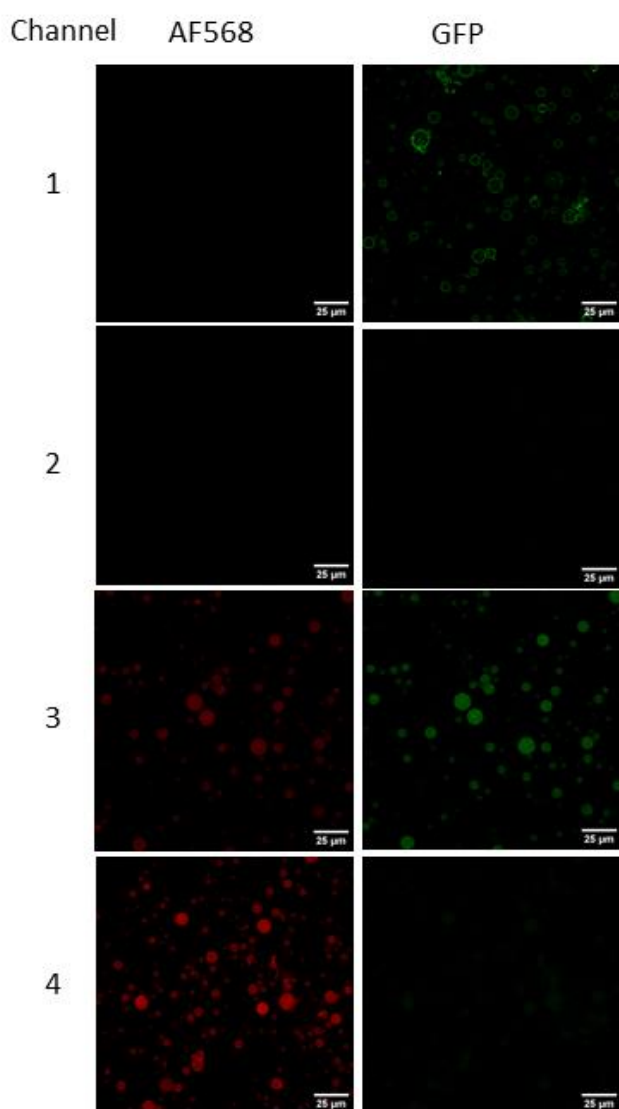


Figure 5 Confocal microscopy images of different samples: 1) tau-GFP 2) bivalent tau 3) 14-3-3 γ + tau-GFP 4) 14-3-3 σ + tau-GFP. Concentrations of all compounds used were 100 nM.

After the experiments in buffer solution and the conformation that proteins can enter the coacervates, it was possible to conduct the first assays in coacervates. The results of the first FP assays in coacervates can be seen in figure 6. This experiment is a 14-3-3 titration that used bivalent tau peptide 2 and 183 and deAcFC-A as stabilizers. The anisotropy for the groups with stabilizer is higher than the group without stabilizer, which might indicate that there is a stabilization effect in coacervates, just like in buffer solution. Additional measurements can be found in figures S 18-19. Although no good S-curve was obtained yet and we might be looking at the upper plateau of the binding curve due to the strong binding of bivalent tau peptide 2 to 14-3-3, these results should be interpreted with caution. The experiment was repeated with tau peptide 1 that has a lower affinity for 14-3-3. The results of this assay (figure 7) show an S-curve, but still similar K_D values for the different conditions were obtained. This indicates that there was no stabilization effect. However, the K_D value when no compound is added is 100-fold higher in buffer than in coacervates (4.7 μ M in buffer compared to 58 nM in coacervate). It is possible that the stabilizers did not enter the coacervate, contrary to what was expected, or that not enough compound was added to measure an effect. The figures S20-21 of the additional measurements performed at different time points do show that the apparent K_D lowers over time for all groups, this might be caused by the accumulation of tau peptide in the coacervates overtime. The experiment was repeated with higher compound concentrations of which the results are shown in figure 8 and 9 and their additional figures in figure S22-23.

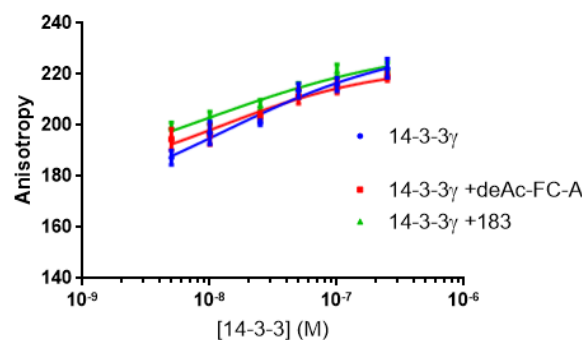


Figure 6 FP assay 14-3-3 γ titration in coacervates at $t=60$ minutes with and without stabilizer. The bivalent tau peptide 2 concentration was 100 nM and stabilizer concentrations of 3.3 μ M were used. Apparent K_D 's could not be estimated

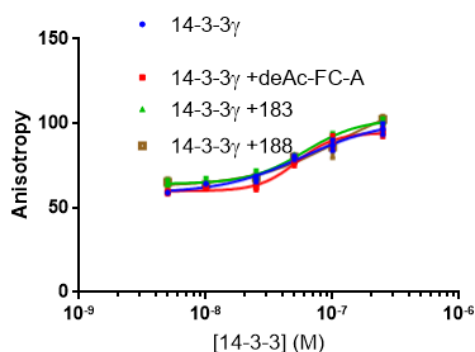


Figure 7 FP assay in coacervates measured at $t= 60$ min. compound concentrations of 3.33 μ M were used. The bivalent tau peptide 1 concentration was 100 nM. Estimated K_D values were 58 \pm 10.9 nM, 52 \pm 4.46 nM, 61 \pm 6.58 nM and 108 \pm 55.4 nM for the groups without compound, with deAc-FC-A, 183 and 188. Peptide concentration was kept constant at 100 nM.

Figure 8 shows another FP assay in coacervates with a higher stabilizer concentration of 25 μM . This assay still does not show a clear stabilization effect. The experiment was repeated one more time with an even higher compound concentration of 250 μM . The results in figure 9 show the top plateaus of the S-curve. This is comparable to when a low compound concentration was used with the different tau peptide. The results indicates that a too high compound concentration was used in this last experiment, and it is hard to conclude whether there is any stabilization effect. Further optimization of this assay is needed, and it is also important to find out whether the stabilizers can enter the coacervates in the first place. This could give an explanation as to why no stabilization effect is observed. It is also possible that the aldehydes precipitate in the coacervates due to their high concentration and bad solubility. The deAc-FC-A results are unexpected in both experiments again. It is suspected that it interacts with the tau peptide in an indirect way, since the FITC signal is also lower compared to the other groups, and that this causes the anisotropy to be lower than expected. The interaction should be indirect, since this effect was not observed in the group with only peptide and deAc-FC-A in the compound titrations in figures S10-14.

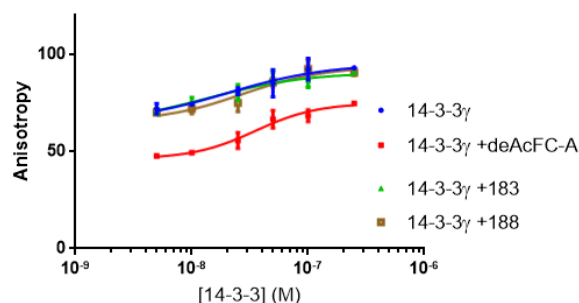


Figure 6 FP assay in coacervates measured at $t=0$ min. compound concentrations of 25 μM were used. The bivalent tau peptide 1 concentration was 100 nM. Estimated K_D values were 20 ± 17.5 nM, 35 ± 6.66 nM, 13 ± 16.4 nM and 27 ± 12.8 nM for the groups without compound, with deAc-FC-A, 183 and 188. Peptide concentration was kept constant at 100 nM.

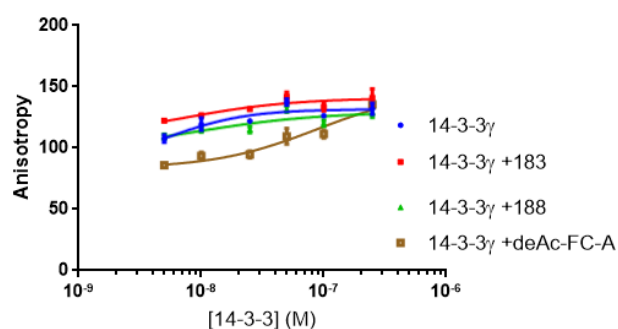


Figure 7 FP assay of 14-3-3 γ titration in coacervates measured overnight. compound concentrations of 250 μM were used. The bivalent tau peptide 1 concentration was 100 nM. K_D values could not be determined.

The first FP assays in coacervates using 14-3-3 σ and bivalent tau peptide 2 have been attempted but have not been successful yet. The results can be found in figure S24. Only the upper plateau of the S-curve was visible, likely because the peptide binds too strongly, the upper part of the curve is already reached even at extremely low 14-3-3 σ concentrations.

FRET (Förster resonant energy transfer) assays to study the 14-3-3/tau binding were also attempted, but no reliable results were obtained, they are depicted in S25-26. They need to be optimized, because they could be an interesting way to study PPIs in coacervates in the future. The FRET signal purely relies on the proximity of the tau peptide and 14-3-3, so their interaction can be

studied more specifically and no other effects would influence the signal^[39]. The FRET ratio was calculated with the relative energy transfer ($E_{\text{rel}} = F_a / (F_d + F_a)$)^[40]. Non-phosphorylated C-Raf was used as an extra control since this peptide does not bind 14-3-3 and it was expected to see no FRET signal for this group. The FRET assays could be optimized by trying another donor and acceptor pair.

Conclusion

In this work, the interaction between 14-3-3 and tau was studied in coacervates. The intrinsic K_D in buffer and apparent K_D in coacervates for the groups without stabilizer using bivalent tau peptide 1 could be compared and went from 4.9 ± 0.584 μM in buffer to 58 ± 10.9 nM in coacervates, which is approximately a 100-fold decrease. This supports the hypothesis that the PPI in coacervates is stronger due to a local higher concentration of the interacting molecules. Furthermore, it has been confirmed by the confocal microscopy images that the tau peptide can enter the protocell model and that this uptake is likely driven by the affinity of the 14-3-3 isoform that is immobilized in the coacervate. However, no significant proof of PPI stabilization of the 14-3-3/tau interaction by deAcFC-A and aldehydes has been observed in coacervates yet. However, the methods used are promising for the future and can be optimized in future research.

Outlook

Interesting results have already been found, although there is still a lot of work to do to truly find out more about PPI stabilization in coacervates. Optimizing the assays performed could be a first step that includes testing with different protein and compound concentrations. The choice was made to continue experiments with a weaker binding tau peptide, but the assays should be optimized such that S-curves can also be obtained using the stronger binding bivalent tau peptide 2 that covers more of the 14-3-3 binding pocket. Apart from this, further development of FRET assays could be an interesting method to study the PPI in coacervates. FRET and Homogeneous Time Resolved Fluorescence (HTRF) could be an interesting method to study the interaction in coacervates because both 14-3-3 and peptide would be labeled, and a signal would only be measured if they are in proximity of each other and the shift in signal could only be due to a stabilization effect. A method should be developed where the stabilizer can enter the coacervate, and that this can be tracked. A possibility is to spin the sample, collect the pellet and study it via LCMS to see if any stabilizer was in the coacervates. Another interesting point of research could be conducting assays with another crowding agent to find out what the effect of soft interactions with the polymer and increased viscosity is and to compare this effect to the increased local concentration in coacervates and buffer. Furthermore, there was no opportunity to conduct experiments with the 14-3-3 ζ isoform and most experiments could not be performed with 14-3-3 σ , which should both taken into consideration in further research. Especially 14-3-3 ζ would be interesting to study in the cell-like coacervates since this isoform is also the most abundant in the brain. It would also be interesting to study the stabilization effect that the compounds have on monovalent tau peptides and full-length tau in the future. It has already been shown that full-length tau can be loaded in the coacervates, so this model could be a good method to study the interaction of full-length tau with 14-3-3 and stabilizers. This study demonstrated that it is interesting and possible to study PPIs in protocells that mimic the crowded environment of the cell's cytosol. There is a lot of potential for future research and still some steps to take to be able to utilize this system as a method for PPI stabilizer screening.

Materials and methods

Compounds

His-tagged 14-3-3 γ , compound 183, 188, dFC-A bivalent tau 1 and 2, Q-Am, Cm-Am, terpolymer and NTA-Am were provided.

Coacervate preparation

To prepare the coacervates, the terpolymer was sonicated for 10 minutes (40 Hz, 185W, degas mode). Buffer, Cm-Am stock, Ni²⁺, NTA-Am and BSA were added in a fresh Eppendorf and Q-Am stock was added while shaking the mixture. After 30 seconds the protein was added and the terpolymer stock was added after 6 minutes.

Protein expression and purification

14-3-3 σ was expressed in *Escherichia coli* BL21 (DE3) cells transformed with a pProEx vector with cDNA to express N-terminally His-tagged 14-3-3 σ . An overnight 4x5 mL small culture in LB medium was used to set up a large 2L culture in TB medium. 2 mL of 0.1 mg/mL ampicillin was added to the large culture and it expended until OD 1.2 at 37 °C and 140 rpm. Afterwards, 0.4 mM IPTG was added to induce protein expression. The cultures were incubated at 25 °C and 140 rpm overnight. Cells were harvested by centrifugation and lysed by homogenation. Proteins were purified using a Ni-NTA column and placed in a 10k snakeskin dialysis bag in dialysis buffer and transferred to SEC buffer after 4 hours. The bag was left in the final buffer overnight. After dialysis, the proteins were concentrated using 10k amicon spin filters, aliquoted and flash frozen. They were kept at -70 °C. Results of Q-TOF analysis can be found in figure S 2 and figure S 3. The purified 14-3-3 and 14-3-3 were labeled using AF568 NHS ester dye (10 mg/mL = 10 mM) in DMF.

14-3-3 labeling

The buffer was exchanged using a G-25 column to the coacervate buffer (20 mM HEPES, 100 mM KCl at pH 7.5). Afterwards, a 1.5 molar excess of AF568 NHS ester dye was added and incubated for 3 hours. Afterwards, a G-25 gel filtration column was used to remove unreacted dye and an amicon MWCO 3 kDa spin filter was used as extra clean-up.

FP assays in buffer

The Fluorescently labelled peptides, 14-3-3 protein and fragments (100 mM stock solution in DMSO) were diluted in FP buffer (10 mM Hepes pH 7.5, 150 mM NaCl, 0.1% Tween 20, 1.0 mg mL⁻¹ BSA) to the desired concentrations. The final DMSO concentration was 1%. Fluorescently labelled peptides concentration was 10 nM for bivalent tau peptide 2 and 100 nM for bivalent tau peptide 1. Dilution series of 14-3-3 protein or compounds were made on Corning black, round-bottom, low-binding 384-well plates (Product Number 4511), in a final sample volume of 10 μ L. Polarization was measured with a Tecan Infinite F500 plate reader using appropriate excitation and emission wavelength for FITC (λ_{ex} : 485 nm, λ_{em} : 535 nm). The gain was set manually at 65. FP data were fitted to a four-parameter dose-response curve using Graphpad Prism 5 software (GraphPad Software, San Diego, CA, USA). 14-3-3 titrations were performed with concentrations starting at 400 μ M and compound concentration of 250 μ M. A 2 times dilution was made in each step. Compound titrations were performed with compound concentrations at 1mM and 14-3-3 concentrations equal to the EC₂₀ values (5 nM for 14-3-3 γ and 200 nM for 14-3-3 σ)

FP assays in coacervates

The Fluorescently labelled peptides, 14-3-3 protein and fragments (100 mM stock solution in DMSO) were diluted in coacervate buffer (20 mM HEPES, 100 mM KCl at pH 7.5) to the desired concentrations. Fluorescently labelled peptide concentration was either 10 or 100 nM. Dilution series of 14-3-3 protein or compounds were made on Corning black, round-bottom, low-binding 384-well plates (Product Number 4514), in a final sample volume of 15 μ L. Polarization was measured with a Tecan Infinite F500 plate reader using appropriate excitation and emission wavelength for FITC (λ_{ex} : 485 nm, λ_{em} : 535 nm). FP data were fitted to a four-parameter dose-response curve using Graphpad Prism 5 software (GraphPad Software, San Diego, CA, USA). The 14-3-3 γ titrations were carried out with concentrations of 0, 5, 10, 25, 50, 100 and 250 nM and compound concentrations of either 10 μ M or 250 μ M.

FRET assays in buffer

The Fluorescently labelled peptides, 14-3-3 protein and fragments (100 mM stock solution in DMSO) were diluted in FP buffer (10 mM Hepes pH 7.5, 150 mM NaCl, 0.1% Tween 20, 1.0 mg mL⁻¹ BSA) to the desired concentrations. The final DMSO concentration was 1%. Fluorescently labelled peptides concentration was 10 nM. Dilution series of 14-3-3 protein or compounds were made on Corning black, round-bottom, low-binding 384-well plates (Product Number 4511), in a final sample volume of 10 μ L. FRET signal was measured with a Tecan Infinite F500 plate reader using appropriate excitation and emission wavelength for FITC (λ_{ex} : 485 nm, λ_{em} : 535 nm). Data were fitted to a four-parameter dose-response curve using Graphpad Prism 5 software (GraphPad Software, San Diego, CA, USA). 14-3-3 titrations were performed with concentrations starting at 400 μ M and compound concentration of 250 μ M. A 2 times dilution was made in each step. C-raf and tau peptide concentrations were 10 nM.

SDS-PAGE

Took 10 μ L samples of supernatant, wash, elution fractions and combined them with 1M DTT with SDS sample buffer. Heated the samples to 95 °C for 10 minutes. Loaded 12 μ L of sample into separate slots and added 6 μ L of ladder. Ran the gel for 60 minutes and washed with MO, stained with Coomassie and destained with MQ. A picture was taken after destaining overnight.

Q-TOF

Purity and exact mass of rhodamine labelled 14-3-3 σ/γ was determined using a High-Resolution LC-MS system consisting of a Waters ACQUITY UPLC I-Class system coupled to a Xevo G2 Quadrupole Time of Flight (Q-ToF). The system was comprised of a Binary Solvent Manager and a Sample Manager with Fixed-Loop (SM-FL). The protein was separated (0.3 mL min⁻¹) by the column (Polaris C18A reverse phase column 2.0 x 100 mm, Agilent) using a 15% to 75% acetonitrile gradient in water supplemented with 0.1% v/v formic acid before analysis in positive mode in the mass spectrometer. Deconvolution of the m/z spectra was performed using the MaxENTI algorithm in the Masslynx v4.1 (SCN862) software.

Confocal microscopy

For analysis, 100 μ L of each coacervate sample was loaded on an 18 well glass bottom microscopy slide (Ibidi). Imaging of coacervates was performed using a Leica TCS SP5 confocal microscope equipped with an HCX PL Apo CS 63x/1.20 UV-vis-

IR water-immersion objective and hybrid detector. The pinhole was set to 1 Airy Unit. Images (1024×1024 pixels) were acquired with a scan rate of 100 Hz and line averaging of 4 times. FAM and GFP were excited at 488 nm (5% laser power), and emission was recorded between 508 and 538 nm. AF568 was excited at 552 nm (10% laser power), and emission was recorded between 570–600 nm. Detector gain was optimized for dynamic range and kept constant between samples with equal concentration (i.e. all samples with 100 nM peptide).

References

- [1] J. de Las Rivas, C. Fontanillo, *PLoS Comput. Biol.* **2010**, *6*, 1–8.
 [2] J. J. Heinisch, R. Brandt, *Microb. Cell* **2016**, *3*, 135–146.
 [3] L. Buée, T. Bussière, V. Buée-Scherrer, A. Delacourte, P. R. Hof, *Brain Res. Rev.* **2000**, *33*, 95–130.
 [4] J. F. Neves, O. Petřvalská, F. Bosica, F. X. Cantrelle, H. Merzougui, G. O'Mahony, X. Hanouille, T. Obšil, I. Landrieu, *FEBS J.* **2021**, *288*, 1918–1934.
 [5] M. Hashiguchi, K. Sobue, H. K. Paudel, *J. Biol. Chem.* **2000**, *275*, 25247–25254.
 [6] Y. Joo, B. Schumacher, I. Landrieu, M. Bartel, C. Smet-Nocca, A. Jang, H. S. Choi, N. L. Jeon, K. A. Chang, H. S. Kim, C. Ottmann, Y. H. Suh, *FASEB J.* **2015**, *29*, 4133–4144.
 [7] J. Neddens, M. Temmel, S. Flunkert, B. Kerschbaumer, C. Hoeller, T. Loeffler, V. Niederkofler, G. Daum, J. Attems, B. Hutter-Paier, *Acta Neuropathol. Commun.* **2018**, *6*, 52.
 [8] K. Iqbal, F. Liu, C.-X. Gong, I. Grundke-Iqbal, *Curr. Alzheimer Res.* **2010**, *7*, 656.
 [9] C. Bancher, C. Brunner, H. Lassmann, H. Budka, K. Jellinger, G. Wiche, F. Seitelberger, I. Grundke-Iqbal, K. Iqbal, H. M. Wisniewski, *Brain Res.* **1989**, *477*, 90–99.
 [10] S. Lim, M. M. Haque, D. Kim, D. J. Kim, Y. K. Kim, *Comput. Struct. Biotechnol. J.* **2014**, *12*, 7–13.
 [11] X. Yang, W. H. Lee, F. Sobott, E. Papagrigoriou, C. V. Robinson, J. G. Grossmann, M. Sundström, D. A. Doyle, J. M. Elkins, *Proc. Natl. Acad. Sci. U. S. A.* **2006**, *103*, 17237.
 [12] B. Cornell, K. Toyo-oka, *Front. Mol. Neurosci.* **2017**, *10*, 318.
 [13] A. Sengupta, J. Liriano, E. A. Bienkiewicz, B. G. Miller, J. H. Frederich, *ACS Omega* **2020**, *5*, 25029–25035.
 [14] H. Hondermarck, *Handb. Cell Signaling, 2/e* **2010**, *2*, 1367–1374.
 [15] B. Coblitz, M. Wu, S. Shikano, M. Li, *FEBS Lett.* **2006**, *580*, 1531–1535.
 [16] G. Sadik, T. Tanaka, K. Kato, H. Yamamori, B. N. Nessa, T. Morihara, M. Takeda, *J. Neurochem.* **2009**, *108*, 33–43.
 [17] G. Tzivion, J. Avruch, *J. Biol. Chem.* **2002**, *277*, 3061–3064.
 [18] A. Ballone, F. Centorrino, C. Ottmann, *Mol. A. J. Synth. Chem. Nat. Prod. Chem.* **2018**, *23*, DOI 10.3390/MOLECULES23061386.
 [19] N. N. Sluchanko, N. B. Gusev, *J. Alzheimers. Dis.* **2011**, *27*, 467–476.
 [20] Y. Chen, X. Chen, Z. Yao, Y. Shi, J. Xiong, J. Zhou, Z. Su, Y. Huang, *J. Mol. Neurosci.* **2019**, *68*, 620–630.
 [21] A. Salehi-Reyhani, O. Ces, Y. Elani, *Exp. Biol. Med.* **2017**, *242*, 1309–1317.
 [22] C. Xu, S. Hu, X. Chen, *Mater. Today* **2016**, *19*, 516–532.
 [23] P. Stano, P. L. Luisi, *Curr. Opin. Biotechnol.* **2013**, *24*, 633–638.
 [24] P. Walde, *Bioessays* **2010**, *32*, 296–303.
 [25] R. J. Ellis, *Curr. Opin. Struct. Biol.* **2001**, *11*, 114–119.
 [26] A. F. Mason, B. C. Buddingh, D. S. Williams, J. C. M. Van Hest, *J. Am. Chem. Soc.* **2017**, *139*, 17309–17312.
 [27] W. J. Altenburg, N. A. Yewdall, D. F. M. Vervoort, M. H. M. E. van Stevendaal, A. F. Mason, J. C. M. van Hest, *Nat. Commun.* **2020**, *11*, 1–10.
 [28] G. Schreiber, *Curr. Opin. Struct. Biol.* **2002**, *12*, 41–47.
 [29] N. A. Yewdall, B. C. Buddingh, W. J. Altenburg, S. B. P. E. Timmermans, D. F. M. Vervoort, L. K. E. A. Abdelmohsen, A. F. Mason, J. C. M. van Hest, *ChemBioChem* **2019**, *20*, 2643–2652.
 [30] A. Bhattacharya, Y. C. Kim, J. Mittal, *Biophys. Rev.* **2013**, *5*, 99–108.
 [31] B. Köhn, P. Schwarz, P. Wittung-Stafshede, M. Kovermann, *Sci. Reports* **2021**, *11*, 1–15.
 [32] G. Sadik, T. Tanaka, K. Kato, K. Yanagi, T. Kudo, M. Takeda, *Biochem. Biophys. Res. Commun.* **2009**, *383*, 37–41.
 [33] J. Ohkanda, <https://doi.org/10.1246/cl.200670> **2020**, *50*, 57–67.
 [34] P. J. Cossar, M. Wolter, L. Van Dijk, D. Valenti, L. M. Levy, C. Ottmann, L. Brunsveld, *Cite This J. Am. Chem. Soc.* **2021**, *143*, 8454–8464.
 [35] D. G. Priest, L. Cui, S. Kumar, D. D. Dunlap, I. B. Dodd, K. E. Shearwin, *Proc. Natl. Acad. Sci. U. S. A.* **2014**, *111*, 349–354.
 [36] S. Gambaro, C. Talotta, P. Della Sala, A. Soriente, M. De Rosa, C. Gaeta, P. Neri, *J. Am. Chem. Soc.* **2020**, *142*, 14914–14923.
 [37] D. S. H. Chan, M. E. Kavanagh, K. J. McLean, A. W. Munro, D. Matak-Vinković, A. G. Coyne, C. Abell, *Anal. Chem.* **2017**, *89*, 9976–9983.
 [38] Y. Du, S. C. Masters, F. R. Khuri, H. Fu, *J. Biomol. Screen.* **2006**, *11*, 269–276.
 [39] J. A. Broussard, K. J. Green, *J. Invest. Dermatol.* **2017**, *137*, e185.
 [40] “Calculate Resonance Energy Transfer (FRET) Efficiencies - The fluorescence laboratory.,” can be found under <http://www.fluortools.com/software/ae/documentation/tools/FRET>, n.d.

Supplementary information

14-3-3 titration

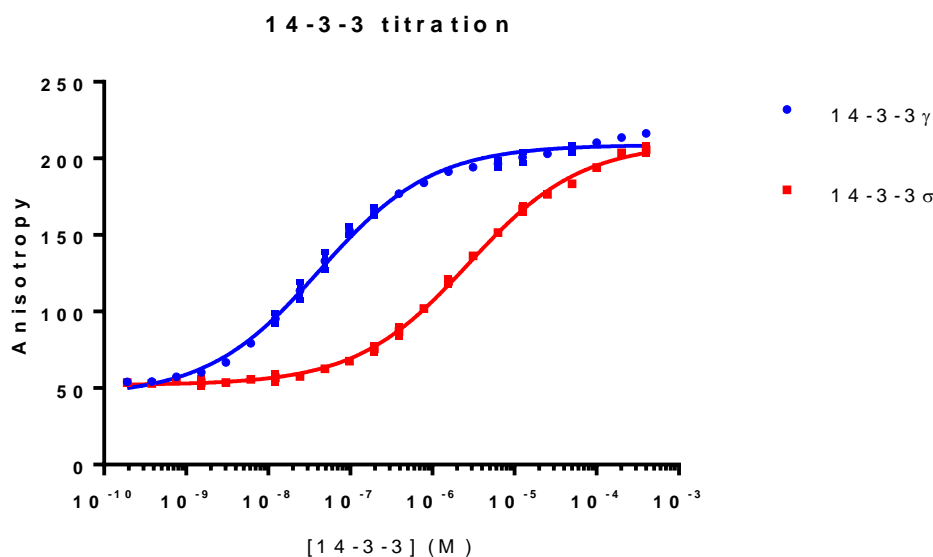


Figure S 1 A titration with 14-3-3 and bivalent tau peptide 2 (10nM) was carried out to determine the K_D of 14-3-3 σ and 14-3-3 γ . Their respective values were measured to be $2.7 \pm 0.281 \mu\text{M}$ and $42 \pm 2.96 \text{ nM}$.

Q-TOF analysis of expressed proteins

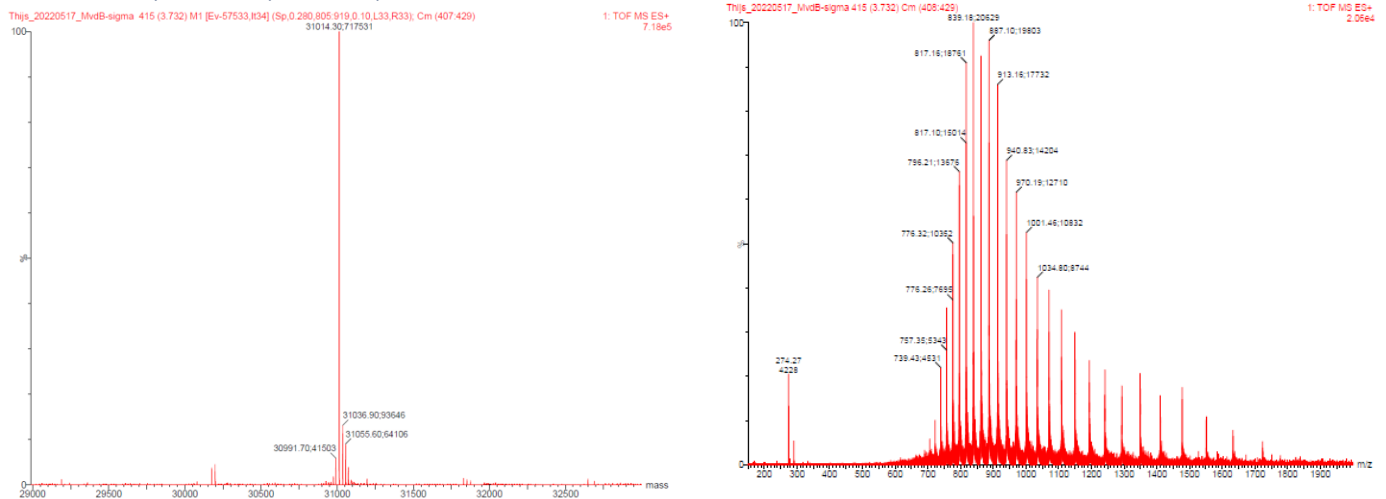


Figure S 2 Deconvoluted image of Q-TOF analysis(left) and full spectrum (right) after purification of the expressed 14-3-3 proteins. The expected mass of 31014 for 14-3-3 σ was measured at 31014.30 and the other peaks can be assigned to the presence of sodium and other minor impurities that could not be determined specifically.

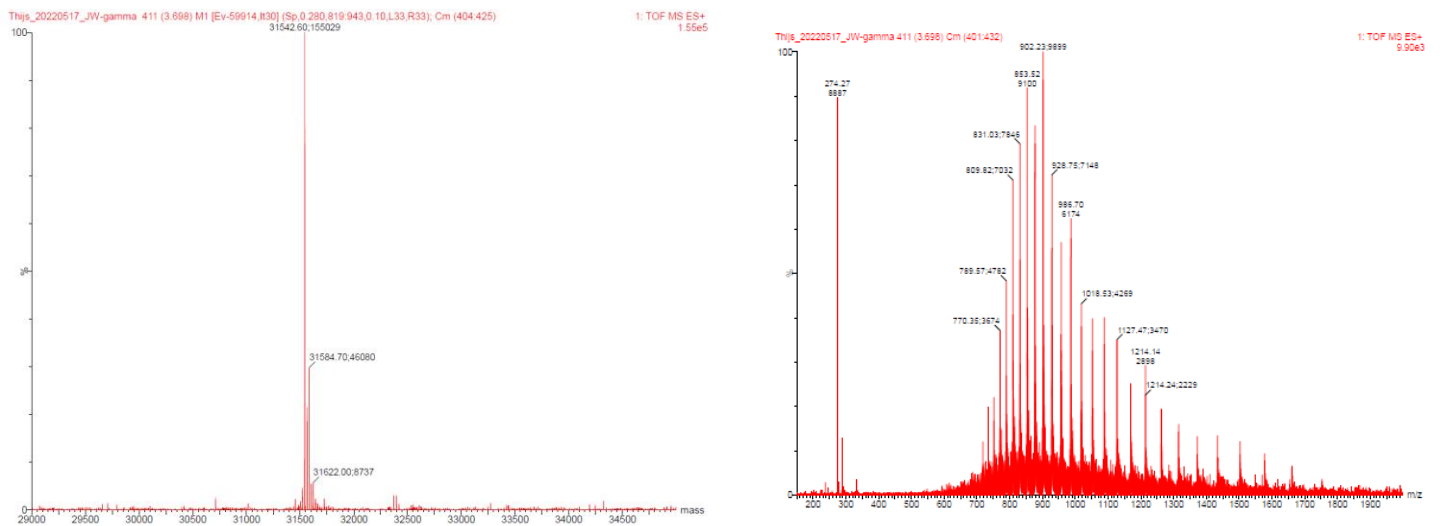


Figure S 3 Deconvoluted image of Q-TOF analysis(left) and full spectrum (right) after purification of the expressed 14-3-3 proteins. The expected mass of 31542 was measured 31542.60 and belongs to 14-3-3 σ and the other peaks can be assigned to the presence of sodium and other minor impurities that could not be determined specifically.

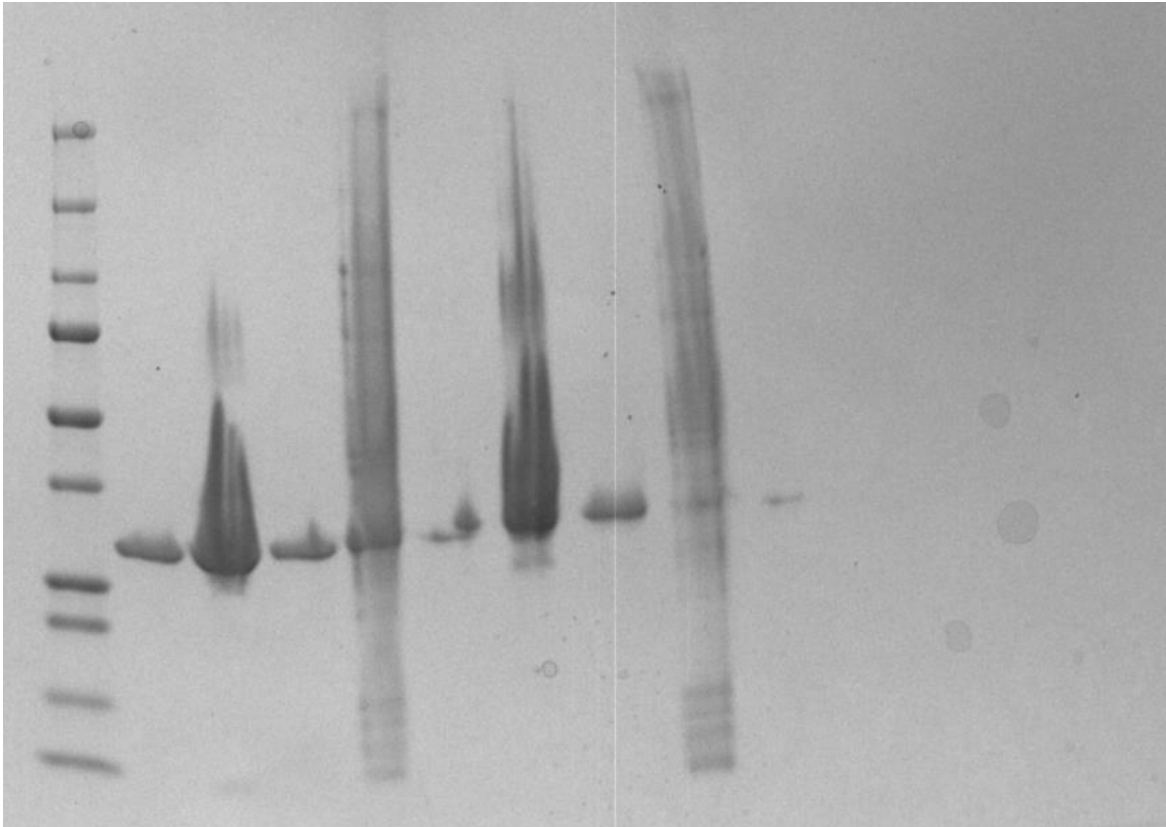


Figure S 4 SDS-PAGE analysis of samples, the gel was loaded as follows (from left to right): 1) ladder, 2) 14-3-3 σ elution fraction 1, 3) 14-3-3 σ elution fraction 2, 4) 14-3-3 σ elution fraction 3, 5) 14-3-3 σ supernatant, 6) 14-3-3 γ elution fraction 1, 7) 14-3-3 γ elution fraction 2, 8) 14-3-3 γ elution fraction 3, 9) 14-3-3 γ supernatant. The gel was overloaded so not clear lines were obtained.

FP assays

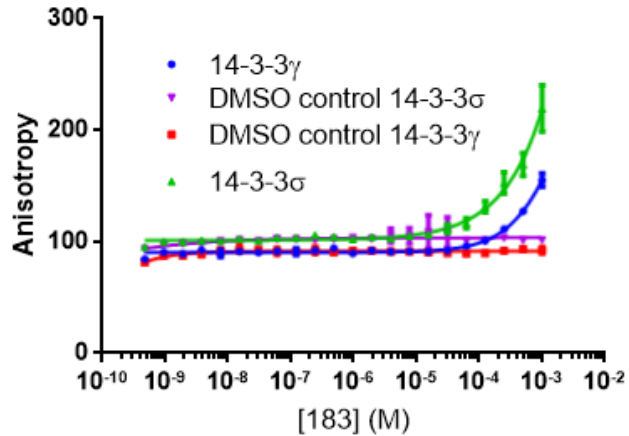


Figure S 5 FP assay measured at $t=0$ minutes, 183 titration with constant 14-3-3 concentration at EC_{20} , 10nM peptide and one percent DMSO 14-3-3 σ concentration was 200 nM and the 14-3-3 γ concentration was 5 nM. 183 was dissolved in DMSO, so a control group without compound, with only DMSO was used. The apparent K_D values could not be determined.

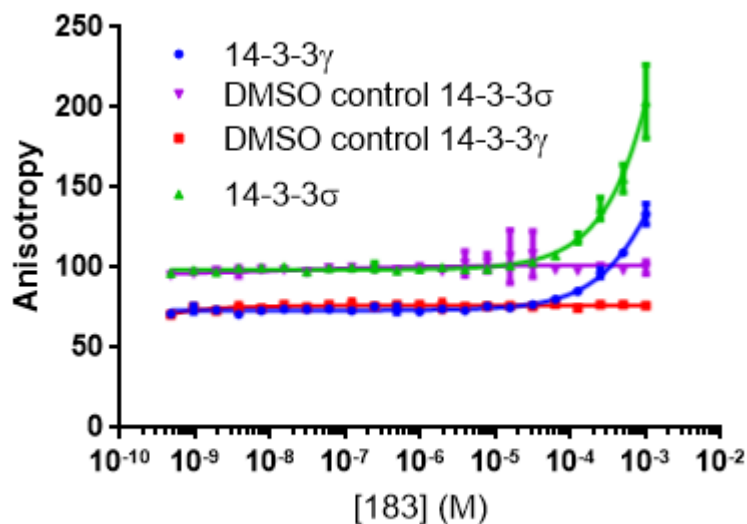


Figure S 6 FP assay measured at $t=60$ minutes, 183 titration with constant 14-3-3 concentration at EC_{20} , 10nM peptide and one percent DMSO 14-3-3 σ concentration was 200 nM and the 14-3-3 γ concentration was 5 nM. 183 was dissolved in DMSO, so a control group without compound, with only DMSO was used. The apparent K_D values could not be determined.

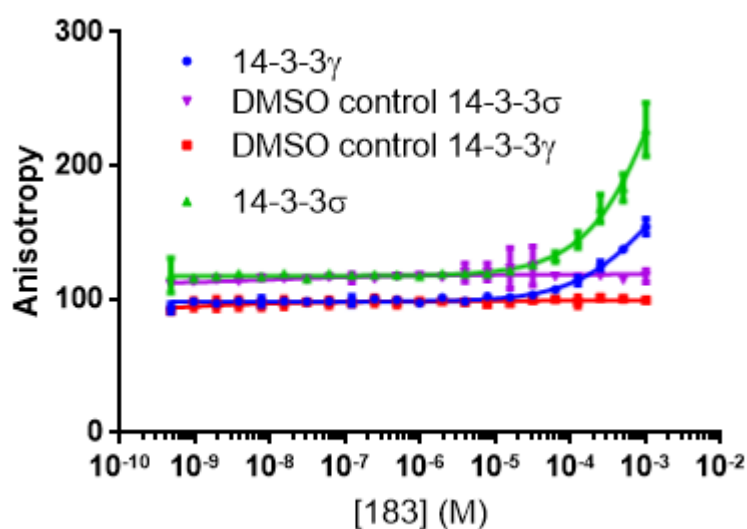


Figure S 7 FP assay measured at $t=120$ minutes, 183 titration with constant 14-3-3 concentration at EC_{20} , 10nM peptide and one percent DMSO 14-3-3 σ concentration was 200 nM and the 14-3-3 γ concentration was 5 nM. 183 was dissolved in DMSO, so a control group without compound, with only DMSO was used. The apparent K_D values could not be determined.

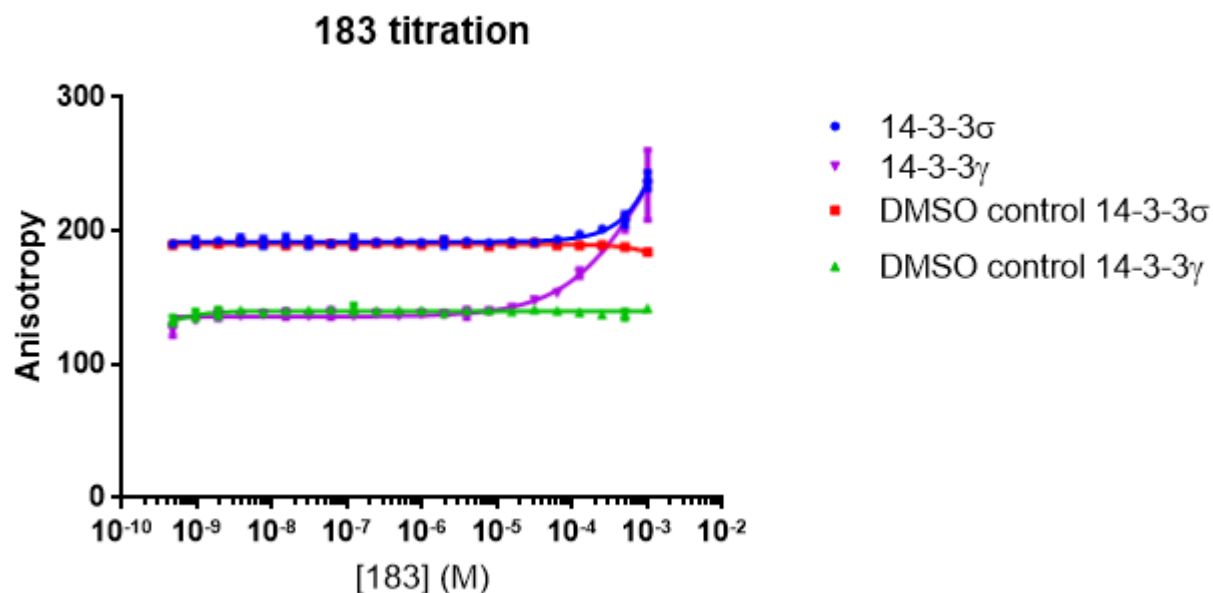


Figure S 8 FP assay measured at $t=180$ minutes, 183 titration with constant 14-3-3 concentration at EC_{20} , 10nM peptide and one percent DMSO 14-3-3 σ concentration was 200 nM and the 14-3-3 γ concentration was 5 nM. 183 was dissolved in DMSO, so a control group without compound, with only DMSO was used. The apparent K_D values could not be determined.

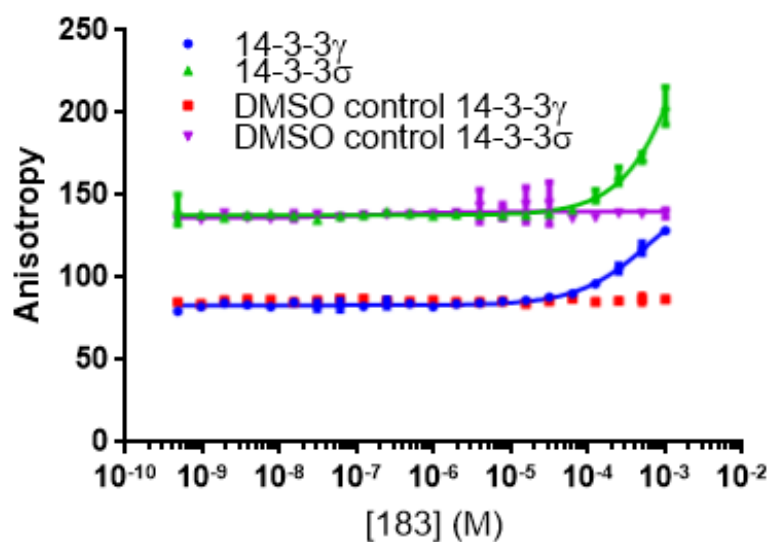


Figure S 9 FP assay measured overnight 183 titration with constant 14-3-3 concentration at EC_{20} , 10nM peptide and one percent DMSO. 14-3-3 σ concentration was 200 nM and the 14-3-3 γ concentration was 5 nM. 183 was dissolved in DMSO, so a control group without compound, with only DMSO was used. The apparent K_D values could not be determined.

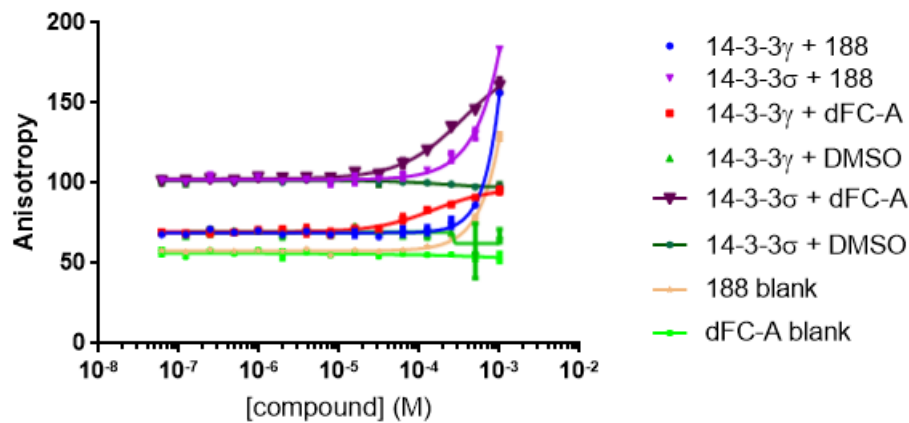


Figure S 10 FP assay measured at $t=0$ minutes of deAcFC-A and 188 titration with a constant 14-3-3 concentration at the EC_{20} for both isoforms, 10nM peptide and one percent DMSO. The apparent K_D values could not be determined.

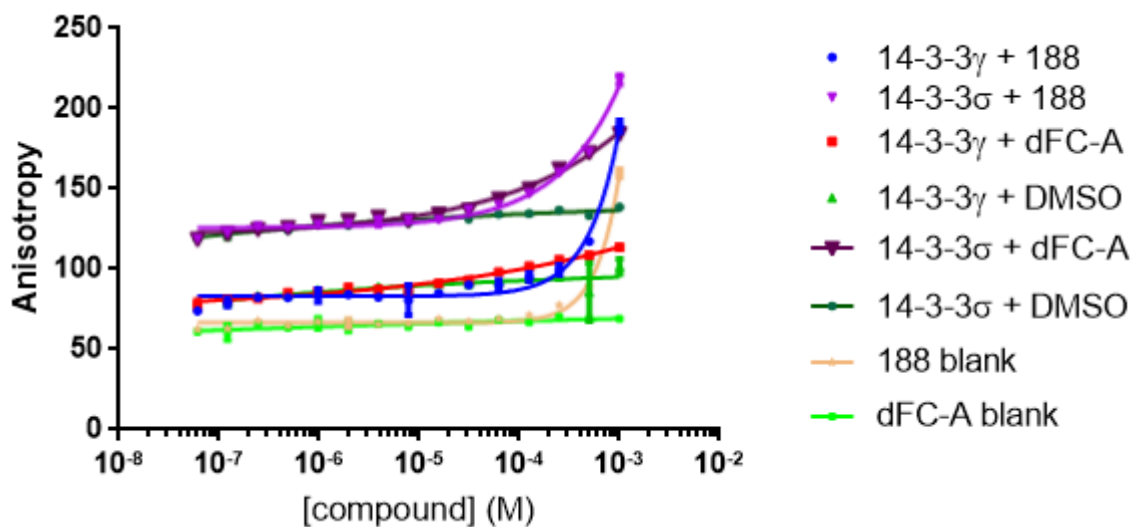


Figure S 11 FP assay measured at $t=60$ minutes of deAcFC-A and 188 titration with a constant 14-3-3 concentration at the EC_{20} for both isoforms, 10nM peptide and one percent DMSO. The apparent K_D values could not be determined.

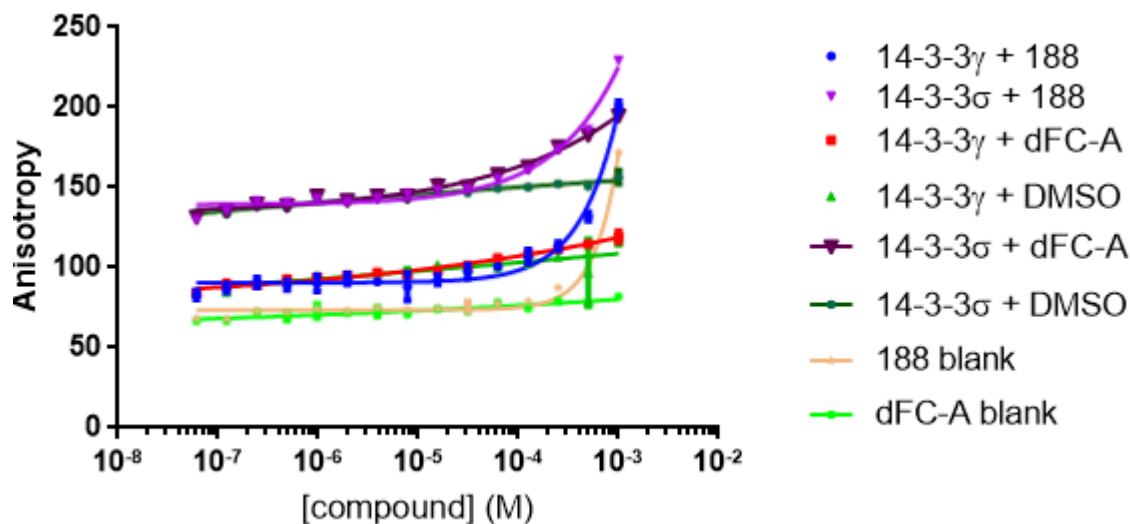


Figure S 12 FP assay measured at $t=120$ minutes of deAcFC-A and 188 titration with a constant 14-3-3 concentration at the EC_{20} for both isoforms, 10nM peptide and one percent DMSO. The apparent K_D values could not be determined.

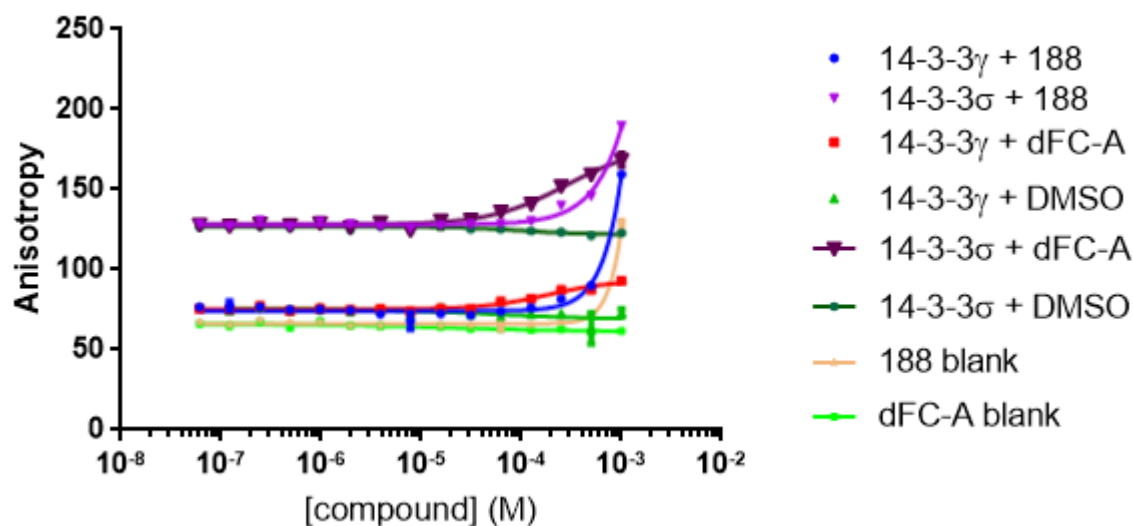


Figure S 13 FP assay measured at $t=180$ minutes of deAcFC-A and 188 titration with a constant 14-3-3 concentration at the EC_{20} for both isoforms, 10nM peptide and one percent DMSO. The apparent K_D values could not be determined.

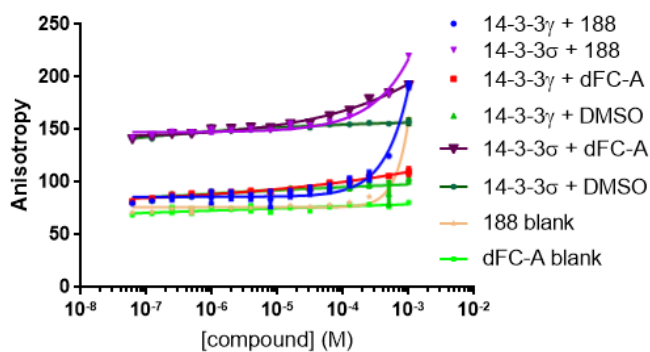


Figure S 14 FP assay measured overnight of deAcFC-A and 188 titration with a constant 14-3-3 concentration at the EC_{20} , 10nM peptide for both isoforms and one percent DMSO. The apparent K_D values could not be determined.

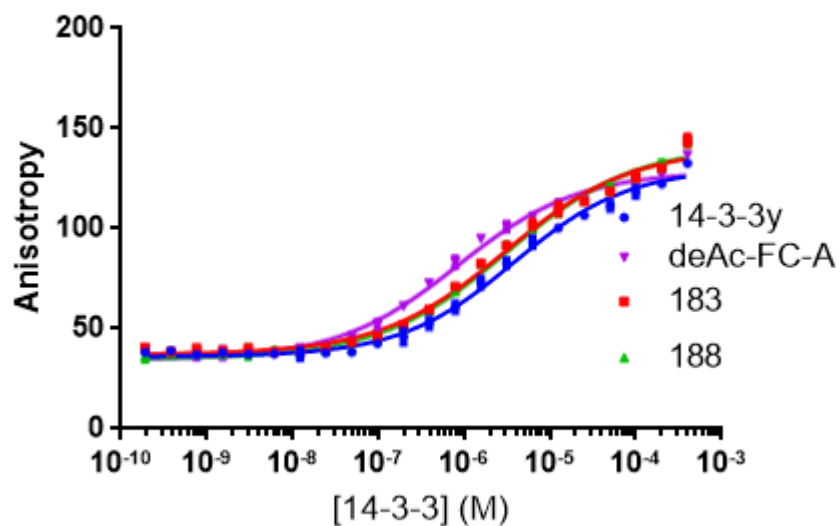
14-3-3 titration

Figure S 15 14-3-3 titration with 250 μ M stabilizer concentration and one percent DMSO measures at $t=60$ minutes. The bivalent tau peptide 1 concentration was 100 nM. The apparent K_D 's were $3.79 \pm 0.348 \mu$ M, $3.0 \pm 0.328 \mu$ M, $3.1 \pm 0.329 \mu$ M and $0.83 \pm 0.080 \mu$ M for the groups without stabilizer, with 183, 188 and deAc-FC-A respectively.

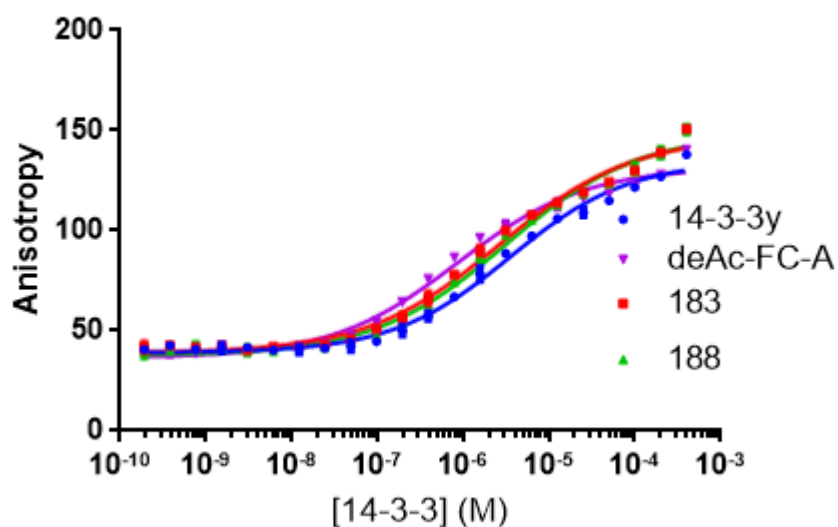
14-3-3 titration

Figure S 16 14-3-3 titration with 250 μ M stabilizer concentration and one percent DMSO measures at $t=120$ minutes. The bivalent tau peptide 1 concentration was 100 nM. The apparent K_D 's were $3.50 \pm 0.374 \mu$ M, $2.6 \pm 0.327 \mu$ M, $3.2 \pm 0.376 \mu$ M and $0.86 \pm 0.091 \mu$ M for the groups without stabilizer, with 183, 188 and deAc-FC-A respectively.

14-3-3 titration

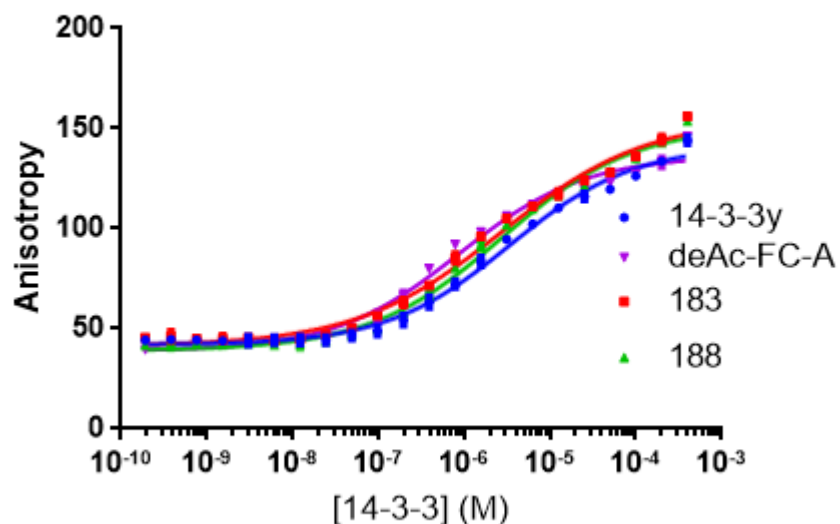


Figure S 17 14-3-3 titration with 250 μ M stabilizer concentration and one percent DMSO measures at $t=180$ minutes. The bivalent tau peptide 1 concentration was 100 nM. The apparent K_D 's were $3.38 \pm 0.380 \mu$ M, $2.7 \pm 0.402 \mu$ M, $2.7 \pm 0.318 \mu$ M and $0.87 \pm 0.101 \mu$ M for the groups without stabilizer, with 183, 188 and deAc-FC-A respectively.

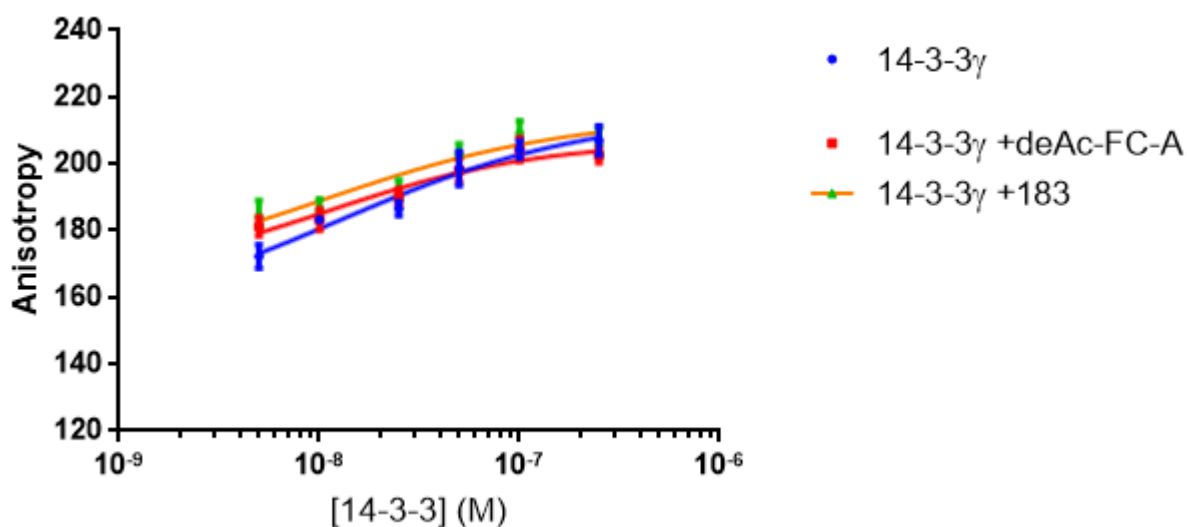


Figure S 18 FP assay 14-3-3 γ titration in coacervates at $t=0$ minutes with and without stabilizer. The concentration deAc-FC-A or 183 used was constant and 3.33 μ M. Bivalent tau peptide 2 concentration was 100 nM. The apparent K_D values could not be determined.

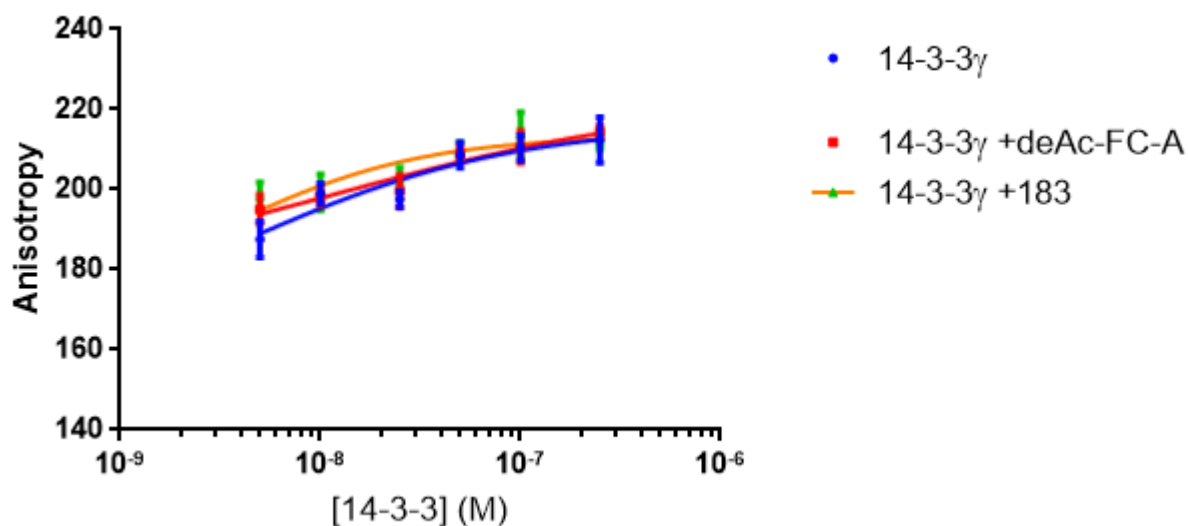


Figure S 19 FP assay 14-3-3 γ titration in coacervates at $t=0$ minutes with and without stabilizer. The concentration deAc-FC-A or 183 used was constant and 3.33 μM . Bivalent tau peptide 2 concentration was 100 nM. The apparent K_D values could not be determined.

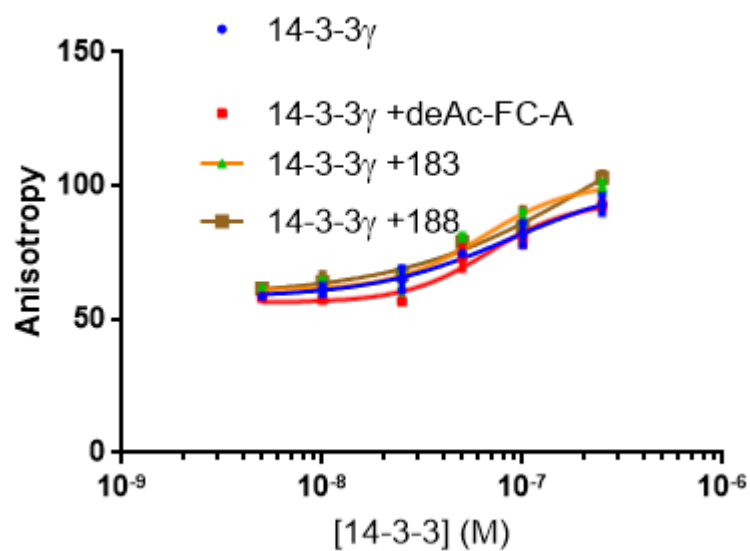


Figure S 20 FP assay in coacervates measured at $t= 120$ min. compound concentrations of 3.33 μM were used. Estimated K_D values were 87 nM, 67 nM, 63 nM and 227 nM for the groups without compound, with deAc-FC-A, 183 and 188. Peptide 1 concentration was kept constant at 100 nM.

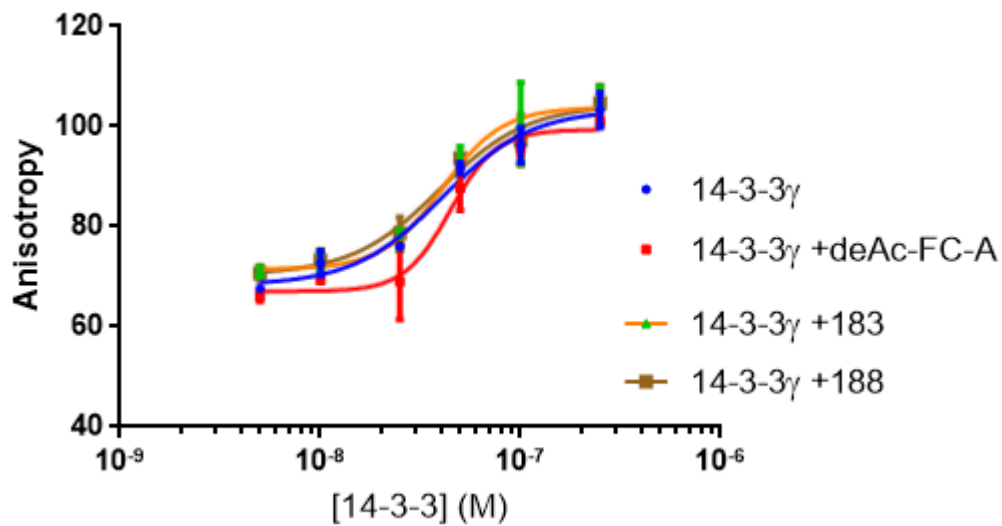


Figure S 21 FP assay in coacervates measured overnight. compound concentrations of $3.33 \mu\text{M}$ were used. Estimated K_D values were $40 \pm 4.7 \text{ nM}$, $44 \pm \text{nM}$, $40 \pm 4.5 \text{ nM}$ and $39 \pm 5.2 \text{ nM}$ for the groups without compound, with deAc-FC-A, 183 and 188. Peptide 1 concentration was kept constant at 100 nM .

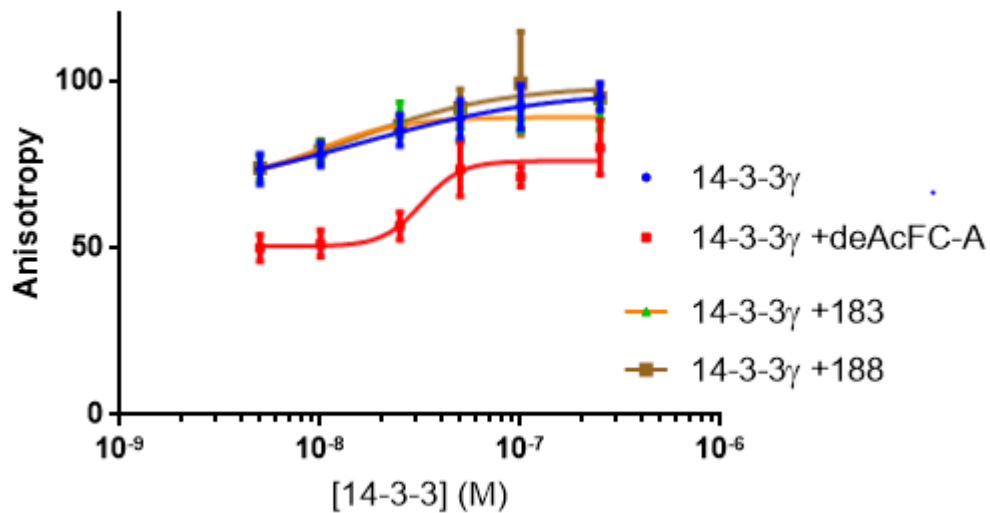


Figure S 22 FP assay of 14-3-3 γ in coacervates measured overnight. A bivalent tau peptide 1 concentration of 100 nM was used and a compound concentration of $25 \mu\text{M}$ was used. Apparent K_D 's could not be estimated from this experiment.

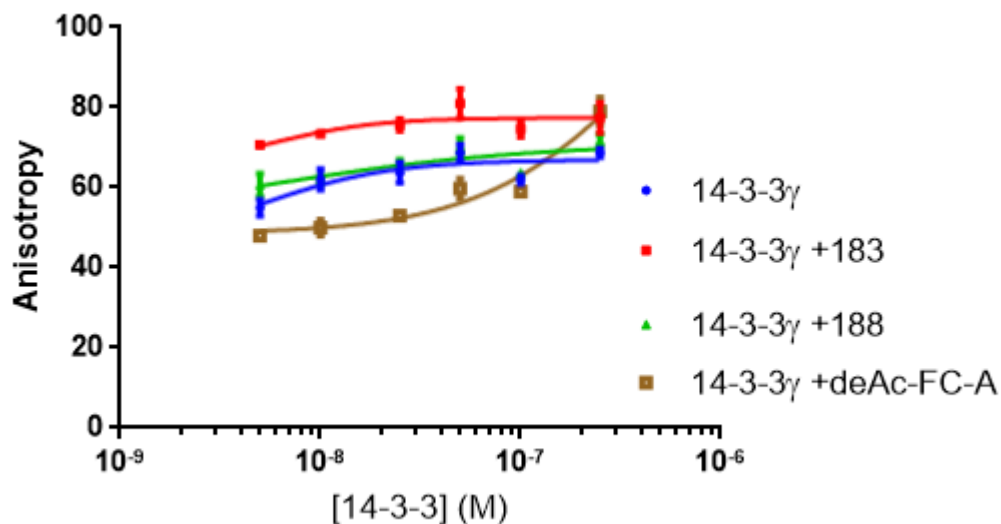


Figure S 23 FP assay of 14-3-3 γ titration in coacervates measured at $t=0$ minutes. compound concentrations of 250 μM were used. The bivalent tau peptide 1 concentration was 100 nM. The apparent K_D values could not be determined.

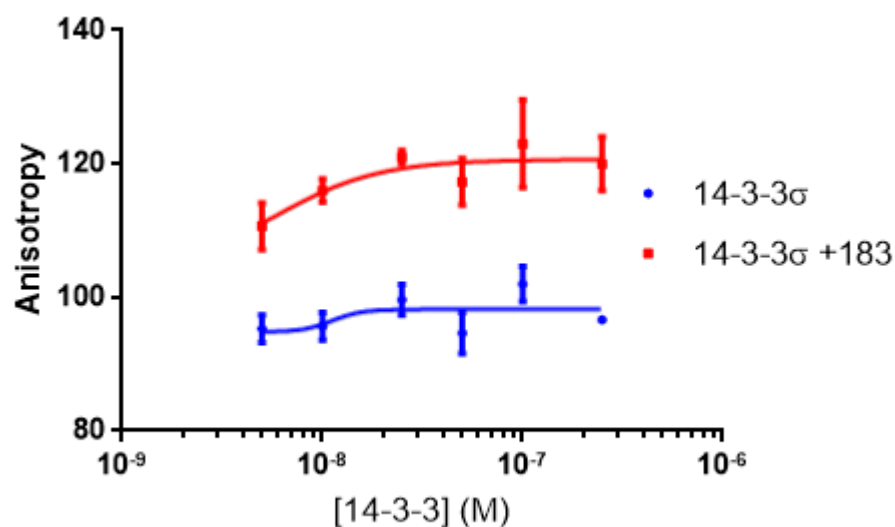


Figure S 24 FP assay of a 14-3-3 σ titration in coacervates with a 100 nM concentration of bivalent tau peptide 2 and 25 μM concentration of 183 compound was used. No apparent K_D could be determined from this experiment.

FRET assays

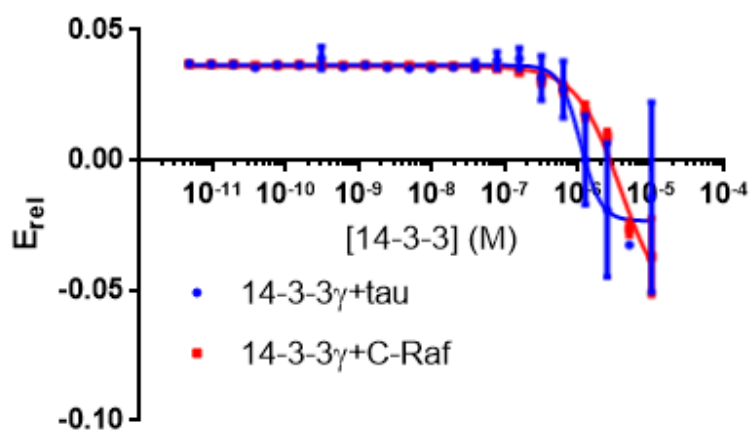


Figure S 25 FRET assay of 14-3-3 γ titration to bivalent tau peptide 2 and C-Raf, both with a concentration of 10 nM.

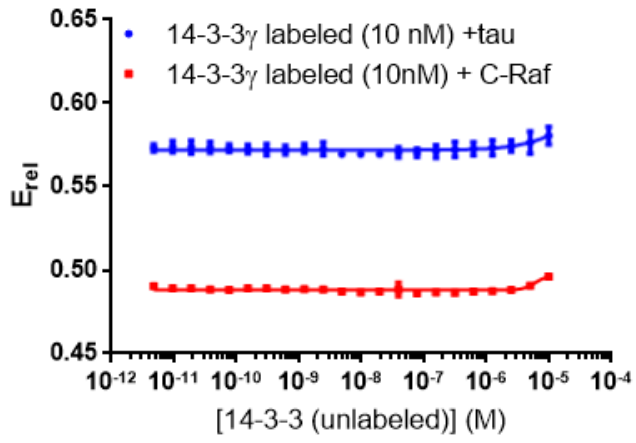


Figure S 26 FRET assay of (non-labeled) 14-3-3 γ titration to bivalent tau peptide 2 and C-Raf with labeled 14-3-3 γ , all with concentration of 10 nM.